JOURNAL OF MATERIALS SCIENCE 17 (1982) 2481–2485

Some geometrical observations on crack front profiles in PMMA double torsion specimens

B. STALDER, H. H. KAUSCH
Laboratoire de polymères, École Polytechnique Fédérale de Lausanne, 32 Chemin de Bellerive, 1007 Lausanne, Switzerland

The double torsion (DT) technique has proved its usefulness in fracture mechanical testing. Practical considerations make it preferable to other methods in many cases. Nevertheless, it is sometimes considered with reluctance, first because of its curved crack front and secondly because of a misunderstanding of the related problems. Experiments were conducted on polymethylmethacrylate (PMMA) to elucidate the effect of crack velocity and geometry. It was found that the crack front profile does not vary with crack velocity, whereas the geometry of the specimen has a strong influence on it. A simple model is developed, based on a strain fracture criterion. It describes quite well the experimental profiles of PMMA. Crack opening displacement, shear modulus, stress intensity factor and Poisson's ratio are shown to be of importance. The influence of the subcritical crack growth exponent could be effective for some materials but not for PMMA.

Nomenclature

a	Crack length.
C	Compliance of specimens.
d	Thickness of specimens.
d_n	Thickness at groove.
E	Young's modulus.
F, F_1	Geometrical parameters
G	Shear modulus.
G_{Ii}	Energy release rate corresponding to a given crack velocity.
G_0	Minimum value of G_{Ii} for crack propagation.
I_p	Torsional moment of inertia.
K_{Ii}	Stress intensity factor corresponding to a given crack velocity.
m	Subcritical crack growth exponent defined by $v \propto (G_{Ii} - G_0)^m$.
M_t	Moment of torsion.
n	Subcritical crack growth exponent defined by $v \propto K_{Ii}^n$.
N	Point on the neutral axis located in the path of the crack.
P_i	Load corresponding to crack propagation at a given overall velocity.
R, R'	Centres of rotation of the deformed sections of the beams.
t	Time.
$\mathbf{T}$	Translation vector.
u	Axis fixed on the side-surface of one beam, perpendicular to $\overline{R'M'}$.
u, u'	Corresponding points on opposite crack surfaces.
v	Crack velocity.
v_l	Local crack velocity.
v_0	X-component of crack velocity at $u = d_n$.
W	Width of the beam, half of DT specimen width.
W_m	Distance between load application points for a beam.
x, y, z	Laboratory co-ordinate system (see Fig. 1); x is the distance from the plane where $\phi = 0$.
α	Local angle of crack front with axis x.
β	Correction factor for beams in torsion.
ζ	Distance between the two planes of crack.
ζ^*	Distance between the two planes of crack for independent beams with permitted overlap.
ζ_f	Maximum depth of overlap.
ν	Poisson's ratio.
ϕ	Relative angle of torsion.

0022–2461/82/092481–05$03.10/0

1. Introduction

Since Gerry [1] has introduced crack propagation in double torsion (Fig. 1) as an experimental method in fracture mechanics, its usefulness has been recognized for many materials. Successful applications have been made principally with ceramics and brittle or semi-brittle polymers. Three-dimensional finite element analysis [2] supports this.

The advantages over other test methods are numerous. The geometry is simple and machining is limited to a groove along the length of the specimen. Compression loading simplifies handling in an oven or an environmental chamber, and precracking is generally easy. Since the stress intensity factor K_{Ii}, does not depend on crack length, propagation is stable and hence suitable for subcritical crack growth studies. The original analysis assumes that when a crack has partially propagated, the separated parts of the specimen are independent beams in torsion. Elementary mechanics and basic concepts of fracture mechanics lead to the following relationship [3–5]:

$$K_{\mathrm{Ii}} = P_{\mathrm{i}} W_{\mathrm{m}} [2 W d^3 d_{\mathrm{n}} \beta (1-\nu)]^{-1/2}. \qquad (1)$$

In fact, this formula (and the closely related ones found in the referenced literature) is an approximation and some of the inherent assumptions are evidently wrong [6]: the crack front is neither straight nor perpendicular to the main specimen surfaces; the compliance of the non-cracked part of the specimen is not infinitely small, and the two beams do not act independently because of the "overlap" of the two deformed sections. To overcome these difficulties, the derivative of the compliance, $\mathrm{d}C/\mathrm{d}a$, is usually measured experimentally. G_{Ii} or K_{Ii} may then be deduced from:

$$G_{\mathrm{Ii}} = \frac{1}{2} \frac{P_{\mathrm{i}}^2}{d_{\mathrm{n}}} \times \frac{\mathrm{d}C}{\mathrm{d}a}. \qquad (2)$$

Analysis of arrest markings and propagation features on fracture surfaces has led to the conclusion that the crack front is always curved regardless of the material tested (Figs 2 and 3). The shape seems to remain constant while the crack propagates through most of the length of a specimen. The apparent propagation proceeds parallel to the translation vector **T** (Fig. 3). However, the surface features observed on PMMA, epoxide resin (EP) or polyaminobismaleinimide (PABM) are always perpendicular to the local crack front, and one has to conclude that they indicate the actual direction of the local crack front displacement. Consequently the crack speed is not constant over the sample thickness. It can be seen that $v_1 = v_0 \sin\alpha(u)$. It seems to be necessary, therefore, to introduce a correction factor in order to obtain correct velocity data against K_{Ii}. Evans [7] gave such a correction for nearly straight fronts. Pollet and Burns [8] extended this geometrical correction for any curved front by relating the apparent velocity, v_0, to the mean value obtained for G_{Ii}, assuming that the relation $v \propto (G_{\mathrm{Ii}} - G_0)^m$ is valid. Virkar and Gordon [9] stated that a velocity distribution also implies a distribution of K_{Ii}. This assertion comes from the unique relationship between v and K_{Ii} or G_{Ii} demonstrated experimentally [10]. Consequently, a given material in a given environment would provide a crack front profile which diverges from that calculated theoretically using a constant K_{Ii}. With this argument in mind, Virkar and Gordon [9] suggested the subcritical crack growth to be the parameter determining crack front profiles. Trantina [11] then compared the crack profiles of different materials selected from polymers, metals and ceramics with their subcritical crack growth exponent, n (proportionality of v and K_{Ii}^n). No significant trend was found.

One important point must be noted. In all the above investigations [2, 8, 9, 11] it has been implicitly assumed that for a given material a corresponding and unique crack profile existed which was independent of the specimen geometry. If that were the case then a complete $v(K_{\mathrm{Ii}})$-curve should be obtainable by crack profile measurement and correct theoretical evaluation. It is the aim of this paper to test to what extent crack front profiles are really independent of geometry.

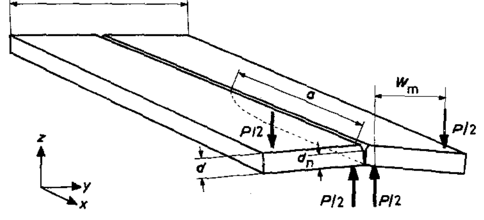

Figure 1 Double torsion specimen.

2. Experimental procedure and observations

2.1. Influence of velocity

All experiments were conducted on PMMA "Plexiglas xt", supplied in the form of sheets by

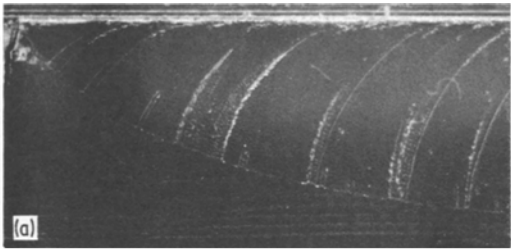

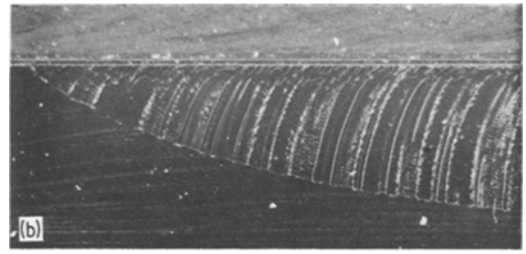

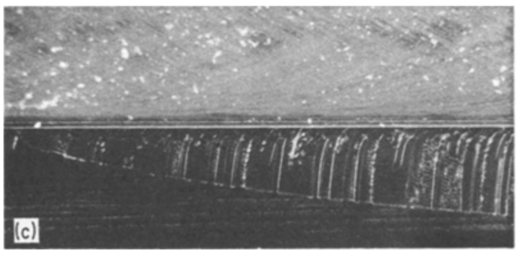

Figure 2 Crack profiles in PMMA with (a) $d = 5.9$ mm, $d_n = 5.55$ mm; (b) $d = 5.9$ mm, $d_n = 4.5$ mm; and (c) $d = 5.9$ mm, $d_n = 3.0$ mm.

Röhm GmbH. The specimens were 5.9 mm thick, 30 mm wide, 60 and 80 mm long. with a 60° V groove 0.9 mm deep. The crosshead speed was varied between 0.05 mm min^{-1} and 50 mm min^{-1}. Crack velocities were approximately two orders of magnitude greater. When about half of the specimen was cracked, a crosshead speed of 1000 mm min^{-1} was applied in the opposite direction to unload the sample. The specimen was then turned and a crack propagated at the opposite end until final fracture occurred. The crack front profiles were thus made visible. The fracture surfaces were photographed and compared. In the range of velocities tested, the crack profiles were nearly identical, no significant change was observed. It might be conjectured that this identity of profiles derives from an immediate adjustment of crack profile to crack speed during the unloading. The arrest lines would then be an equilibrium front corresponding to a slow speed at which K_{Ii} is just insufficient to open the crack further. To elucidate this point, the perpendicular markings produced in the whole velocity range were also checked. Their shape remained constant for all the specimens, indicating that the crack profiles are actually the same in the whole velocity range and not the result of the unloading procedure.

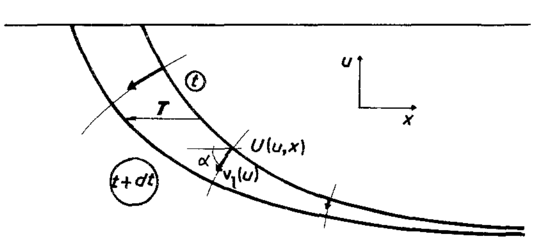

Figure 3 Schematic representation of the propagation of a DT curved crack.

2.2. Influence of geometry

Specimens 30 mm wide and 77 mm long were cut into plates 5.9 and 3.0 mm thick, respectively. They were sidegrooved (this time by a U-groove 0.5 mm wide) in order to obtain d_n equal to 5.55, 4.5, 3.0 and 1.45 mm for the first series and 2.65 and 1.65 mm for the second. A reference crosshead speed of 0.5 mm min^{-1} was chosen. The crack velocity v_0 was not exactly the same for all the specimens because of the different geometries. This is not important, since the profiles are independent of velocity. The unloading procedure was as described above. The profiles were compared in different co-ordinate axes (x, u), $(x/d, u/d)$, $(x/d_n, u/d_n)$. Attempts to superimpose them were in vain. Fig. 2 presents some examples of specimens 5.9 mm thick with different groove depths.

It must be noticed that the range of crack fronts observed here embodies the extreme profiles given by Trantina [11] for different materials. Thus, geometrical parameters can be preponderant over material characteristics. In the present investigation ruptured specimens of PABM, EP and PMMA seemed to behave very similarly when their geometries were taken into account. Studies on other materials are under way with a fixed geometry. Some problems have been encountered since the needs for grooving are different and sometimes incompatible; for example in PABM a very deep groove is necessary to avoid crack deviation.

3. A simple model to calculate crack front profiles based on strain

Let us imagine a cracked slice removed from a DT specimen, parallel to yz (Fig. 4a and b). We can define the distance, ζ, between the side surfaces of the beams, close to and beyond the deformed crack tip. ζ must be taken as a virtual distance between the extrapolated sides. First the corresponding quantity ζ^* for two independent beams under torsion may be calculated as a function of x and u. Considering Fig. 4b, it may be shown that:

$$\begin{aligned}\zeta^*(u,x) &= MM'(x) + 2c(u,x) \\ &= W(1-\cos\phi) + 2(u-d/2)\sin\phi.\end{aligned} \quad (3)$$

The hatched region represents an overlap which is physically impossible. Referring to Fig. 4, it is seen that the overlap below the point N on the neutral axis of the beams is accommodated by suitable compressive stresses. For simplicity it is assumed that N is situated in the middle of the ligament below the crack tip. This assumption implies that both sections of the beams are translated. A mixed deformation of flexure and warping results. The distance ζ becomes:

$$\zeta = \zeta^* - \tfrac{1}{2}(\zeta^* + \zeta_f) = \tfrac{1}{2}(\zeta^* - \zeta_f). \quad (4)$$

Simple geometrical considerations lead to:

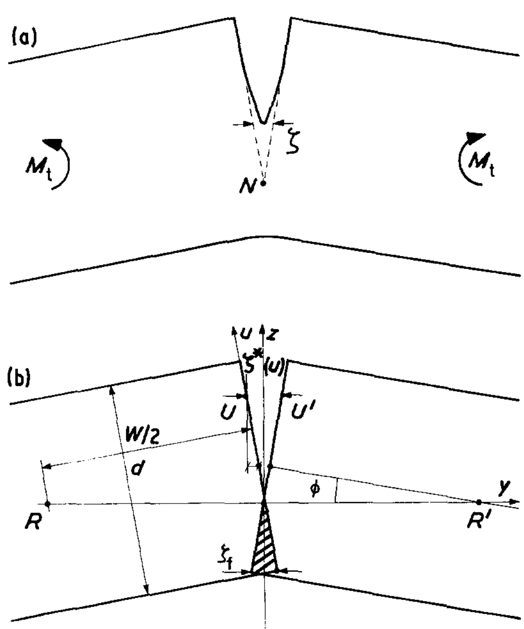

Figure 4 Deformation in a slice of material removed from a DT specimen. (a) Slice with a partial crack. (b) Independent beams in torsion.

$$\zeta^* = W(1-\cos\phi) + 2(u-d/2)\sin\phi \quad (5)$$

and

$$\zeta_f = W(1-\cos\phi) - d\sin\phi. \quad (6)$$

Hence:

$$\zeta = u\sin\phi. \quad (7)$$

As the angle ϕ is small:

$$\zeta = u\phi. \quad (8)$$

Using the results for torsion [12]:

$$\phi = M_t x/GI_p, \quad (9)$$

$$M_t = P_i W_m/2, \quad (10)$$

$$I_p = \beta W d^3, \quad (11)$$

the value of P_i taken from the expression of K_{Ii} (our model is essentially similar to those used to calculate K_{Ii}) is:

$$P_i = (K_{Ii}/W_m) \times [2Wd^3 d_n(1-\nu)\beta]^{1/2}, \quad (12)$$

and setting apart materials characteristics and geometrical factors, we find the sought for expression for the crack front profile, $u(x)$:

$$u = MF/x, \quad (13)$$

with

$$M = \frac{\zeta G}{K_{Ii}(1-\nu)^{1/2}}, \quad (14)$$

and

$$F = \left(\frac{2\beta W d^3}{d_n}\right)^{1/2}. \quad (15)$$

or

$$u/d_n = MF_1/(x/d_n) \quad (16)$$

with

$$F_1 = \left(\frac{2\beta W d^3}{d_n^5}\right)^{1/2} \quad (17)$$

The factor M comprises the quantities G and K_{Ii} which are global material characteristics of a specimen. K_{Ii} denotes in fact the critical state of strain which promotes crack propagation for specific conditions (material, temperature, strain rate, environment). The shear modulus G is defined by the same conditions. The value of ζ is a local deformation parameter which must be distinguished from a crack opening displacement (COD) in that it is the sum of the local plastic strain (COD) and the surrounding elastic strain.

Marshall *et al.* [13] demonstrated that for PMMA the value of COD is a constant over a significant range of temperature (− 190 to 80° C) and crack speed (10^{-2} to 10^2 mm sec^{-1}). Variations of K_{Ii} with these parameters are governed by

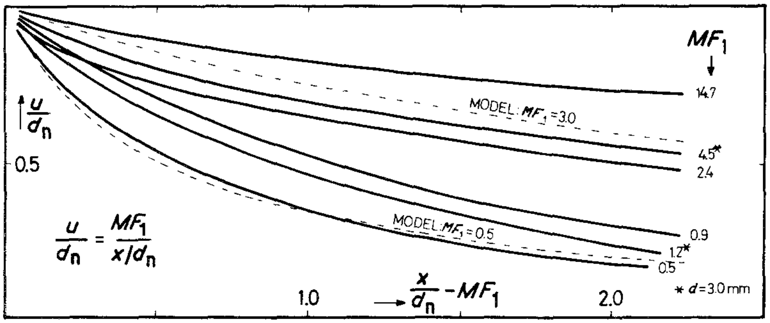

Figure 5 Experimental crack profiles for variables d and d_n with their calculated parameter MF_1 and theoretical profiles (dashed line) given by the model for two values of the parameter.

changes in modulus, keeping the ratio K_{Ii}/E constant. Gledhill and Kinloch [14] arrived at the same conclusions with a particular epoxide adhesive. For PMMA and epoxide resins at least, we may therefore assume that the value of ζ, which is related to the COD, may be taken as a constant. This then defines the relation $u = MF/x$ as the equation of the crack profile.

4. Discussion

The experimental results obtained on PMMA can be compared with the model. For the evaluation the following values were taken: $\zeta = 20\,\mu$m (from a double torsion specimen with $MF_1 = 0.5$); $K_I/E = 3.1 \times 10^{-4}\,\mathrm{m}^{1/2}$ [13]; $\nu = 0.40$; $\beta = 0.29$ for $t = 3.0$ mm and 0.25 for $t = 5.9$ mm; $W =$ 15 mm; d, d_n = as given before, depending on the specimen.

As shown in Fig. 5, there is a strong correlation between calculated and experimental profiles for a fixed sample thickness $d = 5.9$ mm and variable d_n. If, however, the value of d is decreased some differences are observed. This may probably be imputed to the non-cracked part of the specimen, which is not rigid, contrary to the assumption. In fact, its compliance becomes more and more important when d and d_n are decreased. Consideration of this fact would further improve the correspondence.

We wish to conclude this discussion with some remarks concerning possible material influence as related to the factor M. The critical displacement ζ has been taken as a constant. Such a fracture criterion describes well the behaviour of polymethylmethacrylate and epoxide resins but it needs to be proven for other materials before applying the model.

The model may indeed be adapted to other criteria, providing their consequences on the value of M are known. For a material where ζ varies with local crack velocity, crack fronts also depend on the subcritical crack growth exponent. The equation of the profile contains, therefore, a derivative term:

$$ux = M'F \times f\left(\frac{\mathrm{d}u}{\mathrm{d}x}\right). \tag{18}$$

In those cases the model now permits a qualitative interpretation of a crack front profile in double torsion. Theoretical work in this direction and experimental investigations concerning different materials continue in this laboratory.

References

1. D. J. GERRY, PhD thesis, University of Vermont (1966).
2. A. A. TSENG and J. T. BERRY, *J. Press. Vessel Techn.* **101** (1979) 328.
3. J. A. KIES and A. B. J. CLARK, in "Fracture 1969" (Proceedings of the 2nd International Conference on Fracture, Brighton, April 1969) edited by P. L. Pratt (Chapman and Hall, London, 1969) p. 483.
4. R. J. YOUNG and P. W. R. BEAUMONT, *J. Mater. Sci.* **12** (1977) 684.
5. B. J. PLETKA, E. R. FULLER and B. G. KOEPKE, in "Fracture Mechanics Applied to Brittle Materials", ASTM STP 678, edited by S. W. Freiman (American Society for Testing and Materials, 1979) pp. 19–37.
6. E. R. FULLER, Jr, *ibid.*, pp. 3–18.
7. A. G. EVANS, *J. Mater. Sci.* **7** (1972) 1137.
8. J. C. POLLET and S. J. BURNS, *J. Amer. Ceram. Soc.* **62** (1979) 426.
9. A. V. VIRKAR and R. S. GORDON, *ibid.* **58** (1975) 536.
10. G. W. WEIDMANN and W. DOELL, *Colloid Polymer Sci.* **254** (1976) 205.
11. G. G. TRANTINA, *J. Amer. Ceram. Soc.* **60** (1977) 338.
12. S. P. TIMOSHENKO and J. N. GOODIER, "Theory of Elasticity" 3rd edn. (McGraw-Hill Kogakusha Ltd, Tokyo, 1970).
13. G. P. MARSHALL, L. H. COUTTS and J. G. WILLIAMS, *J. Mater. Sci.* **9** (1974) 1409.
14. R. A. GLEDHILL and A. J. KINLOCH, *Polymer* **17** (1976) 727.

Received 30 November 1981
and accepted 19 January 1982